Engineering Journal issn: 0125-8281

Article

Performance Investigation of the Reverse Anoxic/Anaerobic/Oxic Microbial Fuel Cell

Supawadee Siripratum[a] **and Petch Pengchai**[b,*]

The Circular Resources and Environmental Protection Technology Research Unit: CREPT, Environmental Engineering Laboratory, Faculty of Engineering, Mahasarakham University, Thailand
E-mail: [a]61010351004@msu.ac.th, [b,*]petch.p@msu.ac.th (Corresponding author)

Abstract. A reverse anaerobic/anoxic/aerobic (A2O) process is recognized as a developed biological nutrient removal process for wastewater treatment. A few researchers recently integrated a microbial fuel cell (MFC) into an A2O process to generate electricity during wastewater treatment. However, no published studies show the outcome of combining the MFC with the reverse A2O process. The performance of a reverse A2O-MFC during the treatment of raw duck pond water was investigated in this study. For suitable electrode placement, nine patterns of anode and cathode location (CH01-CH09) were also investigated. As a result, 60-79%, 14-52%, 57-82%, and 50-82% of phosphates, nitrates, total ammonia nitrogen, and COD were removed, respectively. Lineweaver-Burk plots could be used to estimate the system's phosphate removal rates. The highest electrical energy was observed at CH05 (162.5 Wh) in the first period of the treatment operation and at CH02 (710.3 Wh) in the second period. The electrode placement patterns of CH05, where the anode and cathode were installed in an anaerobic tank and an oxic tank, and CH02, where the anode and cathode were installed in an anoxic tank and an anaerobic tank, were recommended for the reverse A2O-MFC with a 35-cm electrode distance.

Keywords: Reverse A2O process, microbial fuel cell, electrode distance, phosphate removal, COD removal.

ENGINEERING JOURNAL Volume 26 Issue 10
Received 19 March 2022
Accepted 18 October 2022
Published 31 October 2022
Online at https://engj.org/
DOI:10.4186/ej.2022.26.10.11

1. Introduction

Eutrophication is one of the environmental problems occurring in many parts of the world [1]. It is a condition in which phytoplankton, algae, and aquatic plants overgrow in the water environment, causing oxygen depletion, which kills fish and reduces the recreational and public-utility values of water resources. The main causes of eutrophication are excess nutrient inputs to water bodies from municipal wastewater, industrial discharges, agricultural run-off, construction sites, and urban areas [2]. As a result, a number of environmental engineering disciplines are focusing on the removal of nitrogen and phosphorus from wastewater [3,4].

A biological nutrient removal (BNR), i.e., anaerobic/anoxic/aerobic system (A2O system) in which anaerobic, anoxic, and aerobic processes are combined, is one of the most effective methods for removing nitrogen and phosphorus from wastewater [5]. Phosphorus removal in A2O is dependent on phosphate accumulating organisms (PAOs) via an anaerobic-aerobic sequence in activated sludge processes, whereas nitrogen removal is dependent on groups of bacteria that perform nitrification and denitrification via an oxic-anoxic sequence [5]. Because the anaerobic reactor is located in front of the anoxic phase in the A2O process [6,] a portion of the effluent from an oxic reactor is usually recycled to an anoxic tank to provide a suitable environment for nitrogen removal in the A2O system. However, there is a flaw that frequently reduces the A2O system's nitrogen-removal capacity. The lack of organic substrate for denitrifiers in the anoxic reactor is due to the fact that most of the substrate was previously consumed by PAOs in the anaerobic reactor [5]. To address the shortcomings of the A2O process, a reverse A2O process has been proposed, in which the anoxic reactor is placed before the anaerobic reactor [5]. Both the A2O and reverse A2O systems are said to be excellent organic matter and total nitrogen removers [5]. However, it was demonstrated that lower oxidation-reduction potential in an anaerobic reactor resulted in higher phosphorus uptake in an aerobic reverse A2O reactor [5]. As a result of its superior P removal performance, the reverse A2O process appears to be superior to the A2O process [5].

A microbial fuel cell (MFC) is a promising technology that can generate electricity while biological wastewater treatment is taking place. Microorganisms produce electrons during substrate digestion in the treatment chamber (anode compartment) and then release them outside their cells [7,8]. Some of those electrons are accepted by an electrode (anode) and flow to another electrode (cathode) in another compartment (cathode compartment) [7,8], where they generally react with oxygens and protons to produce water. Several studies [9-11] have recently been conducted by embedding an MFC in an A2O wastewater treatment process to generate electricity during the treatment operation. Because it contained a large amount of organic, an anaerobic tank of the A2O process served as the MFC's anode compartment, while the anoxic tank served as the cathode compartment [9]. Protons generated by activated sludge in the anaerobic tank could flow to the anoxic tank, and the electrons generated as a result are conducted from the anode to the cathode via the external circuit [9]. According to Xie et al. (2013), an MFC embedded A2O reactor (MFC-A2O) with a 6000-ohm internal resistance could produce 14.31.4 mW/m^3 of electricity [8]. It was also demonstrated that the MFC-A2O had higher chemical oxygen demand (COD), total nitrogen (TN), and total phosphorus (TP) removal efficiencies than the control (A2O reactor without embedded MFC) by 15.9%, 9.3%, and 1.4%, respectively [9]. The percentage of *Thauera* and *Emticicia*, identified as denitrifying bacteria, increased significantly in the suspension liquid when the MFC was embedded in the A2O reactor, according to DGGE and Illumina Miseq results [10]. Furthermore, the genus *Rheinheimera* was significantly enriched on the cathode surface, which could help with both nitrogen removal and electricity generation [11].

The above discovery encourages researchers to learn more about MFC-A2O in order to improve BNR technology and increase the process's power output. However, we discovered that a reverse A2O process, which has been shown to be a better phosphorus remover than the A2O process [5], has not been integrated with the MFC technology. As far as we know, no studies on the performance of reverse A2O-MFC have been published. In this study, we designed and built a reverse A2O-MFC. During the treatment of raw duck pond water, we investigated wastewater treatment as well as the power generation of our reverse A2O-MFC. As this is the first step in the reverse A2O-MFC construction, 9 patterns of anode and cathode placement were also investigated to determine the best position for electrode placement.

2. Material and Methods

2.1. Reverse A2O–MFC

As shown in Fig. 1, a reverse A2O system was built that included three continuous stirred-tank reactors (CSTR), namely a 3.33-L anoxic tank, a 5.0-L anaerobic tank, a 26.7-L oxic tank, and an 8.3-L sedimentation tank. Mixing was accomplished using propellers installed at the tops of the anoxic and anaerobic tanks at speeds of 100 and 50 rpm, respectively. Aeration in the oxic tank was accomplished using an aeration pump (HAILEA, model ACO-208). To create a reverse A2O-MFC, electrodes made of 36 cm graphite plates that had previously been heated to 450°C for 30 minutes [12] were installed in the reverse A2O system. Nine patterns of anode and cathode placement were examined to determine the best position for electrode placement. Because of the location of the tanks, these patterns can be divided into three groups, as shown in Fig. 2. Group 1 consisted of three patterns in which cathodes were placed in the anoxic tank and anodes were placed in the anaerobic tank, with anode-cathode pairs separated by 25 cm (CH01), 35 cm (CH02), and 45

cm (CH03) (CH03). Group 2 included three patterns in which cathodes were placed in the oxic tank and anodes were placed in the anaerobic tank, with anode-cathode pairs separated by 25 cm (CH04), 35 cm (CH05), and 45 cm (CH06) (CH06). Group 3 included three patterns in which cathodes were placed in the oxic tank and anodes were placed in the anoxic tank, with anode-cathode pairs separated by 50 cm (CH07), 70 cm (CH08), and 90 cm (CH09) (CH09).

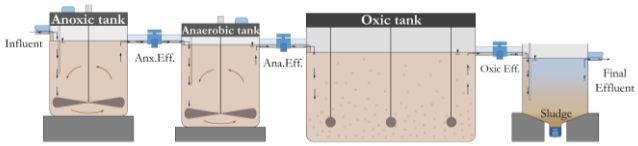

Fig. 1. Reverse A2O–MFC system.

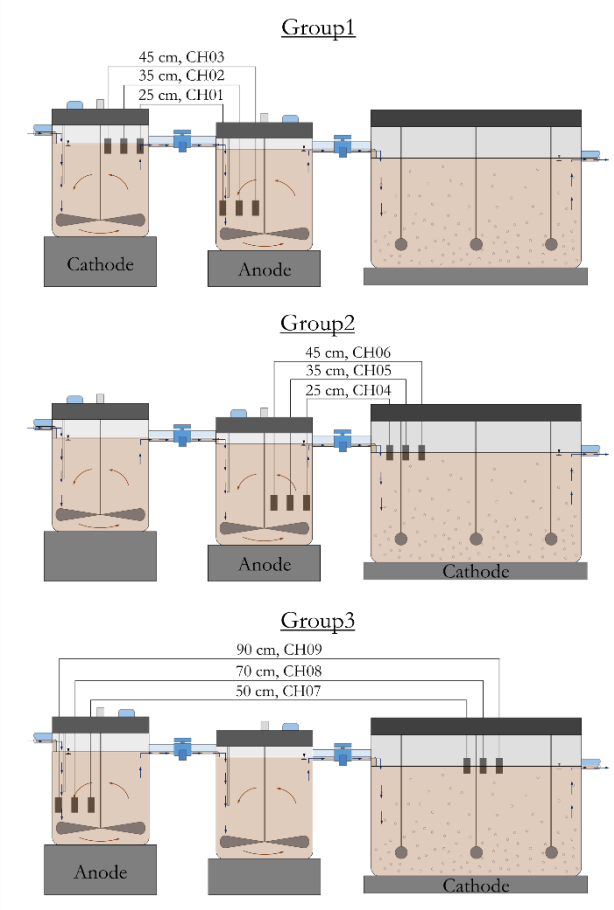

Fig. 2. Electrode-placement patterns in a reverse A2O–MFC system.

2.2. Source of Influent

As an influent of the experiment, water from a eutrophic pond (Fig. 3) in Mr. Khachonsak Saeteng's duck farm in Nonsabaeng village, Kantharawichai city, Mahasarakham province, Thailand was continuously pumped up to the reverse A2O-MFC.

Fig. 3. Source of influent of the reverse A2O–MFC.

2.3. Inoculation Period

The operation was divided into two phases: inoculation and treatment. During the inoculation period, excess sludge from Mahasarakham hospital's activated sludge wastewater treatment system was filled in the anoxic tank, anaerobic tank, and oxic tank to achieve a condition of 3000-mg/l mixed liquor suspended solids (MLSS) in each tank. For 35 days, the sludge was inoculated in each tank by continuously feeding 80 L/d of duck pond water into the reverse A2O-MFC system. The anoxic tank, anaerobic tank, oxic tank, and sedimentation tank had retention times (HRTs) of 1 hour, 1.5 hours, 8 hours, and 2.5 hours, respectively. Because MLSS concentrations in the three tanks were less than 3,000 mg/L, sludge from the sedimentation tank was 100% recycled to the anoxic tank. As a result, the sludge retention time (SRT) during this period was the same as the operation time. Samples were collected at five points in the system (Fig. 1): 1) influent, 2) anoxic tank effluent (Anx.Eff.), 3) anaerobic tank effluent (Ana.Eff.), 4) oxic tank effluent (Oxic.Eff.), and 5) sedimentation tank effluent (Final Effluent), and analyzed for nine parameters listed in Table 1. The Close Reflux Titrimetric Method was used to analyzed the Chemical Oxygen Demand (COD) (Method 5220 C [12]). Total ammonia nitrogen (TAN) analysis was performed using Hach's Nessler method (Method 8038), which was adapted from standard method Method 4500-NH3 [13] and is accepted by the USEPA for wastewater analysis (distillation required) [14]. All water samples were also subjected to nitrate (NO_3^-) analysis using the Phenoldisulphonic method [15], nitrite (NO_2^-) analysis using the Colorimetric method (Methods 4500-[13]), phosphate (PO_4^{3-}) analysis using the Vanadomolybdophosphoric Acid Colorimetric Method (Methods 4500-P [13]), pH analysis using the pH meter, and dissolved oxygen (DO) analysis using the DO meter.

According to Table 1, the system successfully removed phosphate and nitrate while occasionally releasing COD and TAN into the effluent. This could be explained by the fact that the activated sludge in the three tanks was occasionally mixed and dissolved into the water, resulting in higher COD and TAN concentrations in the effluent. However, the system successfully removed 45.0-

50.0% of the COD during the last two days of the inoculation period.

For electricity generation, OCVs were detected at every anode-cathode pair as shown in Table 2. The values ranged from -132 to -3.0 mV at the start and increased to 169.3 to 657 mV at the end of the inoculation period. Because CH04-CH09 had higher OCVs than CH01-CH03, relatively high-power outputs were expected.

2.4. Treatment Period

During the treatment period, the reverse A2O–MFC system was used to treat eutrophic water from the duck pond. The treatment conditions used in this phase, such as flow rate, HRT, sludge recirculation, and sampling points, were the same as those used during the inoculation period. To achieve an MLSS concentration of 3000-mg/L in each of the three tanks, 100% of the removed sludge was continuously recycled to the anoxic tank. As a result, the SRT during this time period was also equal to the operation time. Because the system can generate electricity, the voltages between each anode-cathode pair (CH01-CH09) were measured with a multimeter throughout the experiment (GDM-8255A, Good Will Instrument Co., Ltd.). During the first stage of this treatment period (1st-28th h), each anode-cathode pair was electrically left open without being connected to a resistor. As a result, voltages measured during this stage were dubbed "Open-Circuit Voltage (OCV)." When there was no unexpected decrease in OCV data, a suitable resistor for each anode-cathode pair was defined by the polarization experiment. At the second stage of the treatment period, the anode and cathode terminals of each pair were connected to the selected resistor to create a closed circuit that allowed electrical current to flow between the electrodes. Voltages measured during this stage were called "Closed-Circuit Voltage (CCV)" that can be used for the calculation of power output and electrical energy generated by the reverse A2O–MFC system. The voltages measured during this stage were referred to as "Closed-Circuit Voltage (CCV)," and they can be used to calculate the power output and electrical energy generated by the reverse A2O–MFC system.

Table 2. The potential difference in open-circuit voltage (OCV) format during the inoculation period of the reverse A2O–MFC system.

Placement of electrodes	Potential difference (mV)
CH01	-132.1 – 169.3
CH02	-126.0 – 177.4
CH03	-13.42 – 280.4
CH04	-3.718 – 657.2
CH05	-25.04 – 521.9
CH06	-4.357 – 471.4
CH07	-45.85 – 618.7
CH08	-3.060 – 654.8
CH09	-4.660 – 593.8

Table 1. Water quality during the inoculation period of the reverse A2O–MFC system.

Parameter	Influent	Anx.Eff.	Ana.Eff.	Oxic Eff.	Final Effluent
pH	6.83 ± 0.31	6.86 ± 0.29	6.90 ± 0.26	7.50 ± 0.33	7.42 ± 0.18
DO (mg/L)	0.83 ± 1.80	0.57 ± 0.86	0.47 ± 0.77	6.10 ± 1.02	4.50 ± 1.27
ORP (mV)	–	-21.0 ± 48.6	-45.1 ± 61.1	132 ± 18.9	–
COD (mg/L)	883 ± 311	756 ± 520	679 ± 707	777 ± 703	1110 ± 837
Phosphate (mg/L)	2.25 ± 1.85	2.10 ± 1.74	1.71 ± 0.93	1.37 ± 0.91	1.52 ± 1.22
TAN (mg/L)	3.88 ± 4.80	5.04 ± 5.49	5.53 ± 6.67	4.06 ± 6.41	4.95 ± 5.25
Nitrite (mg/L)	23.0 ± 48.2	14.2 ± 21.8	10.9 ± 16.6	13.0 ± 19.3	10.4 ± 15.4
Nitrate (mg/L)	10.4 ± 12.6	7.88 ± 9.80	7.26 ± 8.98	7.45 ± 8.37	6.46 ± 7.79

2.5. Polarization Experiment

For each anode-cathode pair of the reverse A2O–MFC system, polarization experiments were performed to determine the appropriate resistor that resulted in the highest electrical power output. Various external resistors with resistances (R_{ex}) ranging from 10-60,000 ohms were sequentially connected to each pair of electrodes (5 minutes per each). CCVs were measured across each R_{ex} and used in Eq. (1) to calculate the electrical power (P) transferred to the R_{ex}. The R_{ex} with the highest P for each anode-cathode pair was chosen and used in the treatment operation. Because an electrical condition, such as internal resistance, can change during treatment, a polarization experiment should be performed as frequently as possible to always derive the appropriate R_{ex}. This study conducted two polarization experiments, the first at the end of the first-stage treatment period (29th-30th h) and the second between the 120th and 124th h of the treatment period.

$$P = CCV^2 / R_{ex} \quad (1)$$

2.6. Analysis of Wastewater Treatment Performance

Wastewater treatment performance of the reverse A2O–MFC system was evaluated using pollutant removal efficiencies ($Efficiency_{removal}$,%) calculated in Eq. (2) and pollutant removal rates ($Rate_{removal}$, mg/l"" h) calculated in Eq. (3), where C_{in} is a pollutant concentration in the influent, C_{out} is a pollutant concentration in the final effluent, and HRT_{total} is the sum of HRTs of the three tanks (anoxic tank, anaerobic tank, oxic tank). In this study, removal efficiencies and pollutant concentrations were typically presented as average values ± standard deviations.

$$Efficiency_{removal} = (C_{in} - C_{out}) \times 100 / C_{in} \quad (2)$$

$$Rate_{removal} = (C_{in} - C_{out}) \times 100 / HRT_{total} \quad (3)$$

2.7. Kinetic Analysis of Pollutant Removal Rates

For further understanding of the removal performance, we attempted to estimate our $Rate_{removal}$ data using Lineweaver-Burk plots based on the Michaelis-Menten kinetics equation (Eq. (4) [16]), where Q is the flow rate (L/d), and V is the total volume of the anoxic tank, anaerobic tank, and oxic tank. The linear equation constants defined by regression analysis of the plots are U_{max} (the possible maximum removal rate (mg/l·h)), and K_m (the Michaelis-Menten saturation constant (mg/l)). These calculated kinetic constants should provide more information about the removal performance of our reverse A2O–MFC system.

$$\frac{V}{Q(C_{in} - C_{out})} = \frac{K_B}{U_{max}} \times \frac{V}{QC_{in}} + \frac{1}{U_{max}} \quad (4)$$

2.8. Analysis of Electricity Generation Performance

The reverse A2O–MFC system's electricity generation performance was evaluated using P defined in Eq. (1) and electrical energy (EE) defined in Eq. (5), where t_0 is the initial hour, t_n is the final hour, and n is the number of hourly power output data. As a result, P (W) data represented an hourly capacity of power generation, whereas EE (W·h) data represented the total energy generated by the reverse A2O–MFC during the study period. The power densities produced by the MFCs were calculated by dividing P by an anode area (W/m^2) or an anode chamber volume (W/m^3).

$$EE = \int_{t_0}^{t_n} Pdt = \Sigma_i P_i \times t_i \quad (5)$$

3. Results and Discussion

3.1. Wastewater Treatment Performance

3.1.1. pH, ORP, and DO

Based on 1.412 - 2.258 gCOD/L·d COD loading rates, the average pH for the influent was 6.85±0.15, 6.90±0.11 for the Anx.Eff., 6.89±0.11 for the Ana.Eff., 7.61±0.15 for the Oxic.Eff., and 7.61±0.15 for the Final Effluent during the treatment period. During the operation, the anoxic tank's ORP was -98-72 mV, the anaerobic tank's ORP was -228-66 mV, and the oxic tank's ORP was 70-110 mV. Average DO values for the influent were 2.50±2.21 mg/l, 0.79±0.88 mg/l for the anoxic tank, 0.08±0.06 for the anaerobic tank, 6.05±2.49 for the oxic tank, and 3.24±2.81 for the final effluent. The results showed that the BNR process had acceptable anaerobic conditions for phosphate release (0.1-0.5 mg/l of DO [17]) and oxic conditions for nitrification (2-3 mg/l of DO [18]. However, the average DO in our anoxic tank was higher than the standard denitrification condition (less than 0.2 mg/l of DO [19]). This could result in low nitrate removal efficiency.

3.1.2. Pollutant removal

COD concentrations in the influent ranged from 706±0.00 to 1,129±0.00 mg/l, and our reverse A2O–MFC system removed 50-85% of them (see Fig. 4). However, residual COD concentrations in the final effluent were too high (15912.6 to 4949.8 mg/l) to discharge into inland surface water in accordance with the USEPA standard (250 mg/l [20]). In terms of BNR performance, phosphate concentrations in the influent ranged from 0.42±0.001 to 1.02±0.000 mgP/l, with final effluent concentrations ranging from 0.12±0.009 to 0.29±0.002 mgP/l. Phosphate removal efficiency was achieved at 60-79% (see Fig. 5). Given that the US-EPA recommends TP concentrations of no more than 0.05 mgP/L for streams discharging into reservoirs [21], more work is needed to improve phosphate removal capacity. Higher phosphate concentrations observed in the anaerobic tank (0.51-0.97 $mgPO_4$-P/l) compared to the anoxic tank (0.30-0.53 $mgPO_4$-P/l) on days 6^{th}, 10^{th}, and 12th of the treatment indicated the phosphate-release activity of PAOs in our system. However, possible phosphate removal mechanisms in our oxic tank include PAO phosphate accumulation [5] as well as struvite crystallization, in which phosphate ions precipitate as crystals by binding with positive ions in the water [22]. Ichihashi et al. (2012) used swine wastewater to operate air-cathode MFCs and discovered a large number of struvite crystals accumulated on the cathode surface [23]. The assumption of struvite crystallization had not been proven in our study because there was no inspection of our cathode surface at the time because most of our experimental activities were prohibited during the first COVID-19 epidemics in Thailand.

DOI:10.4186/ej.2022.26.10.11

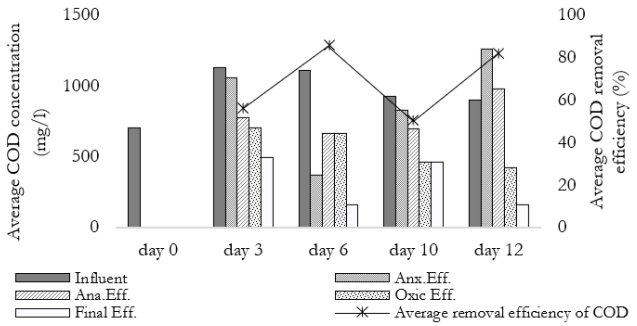

Fig. 4. COD removal performance.

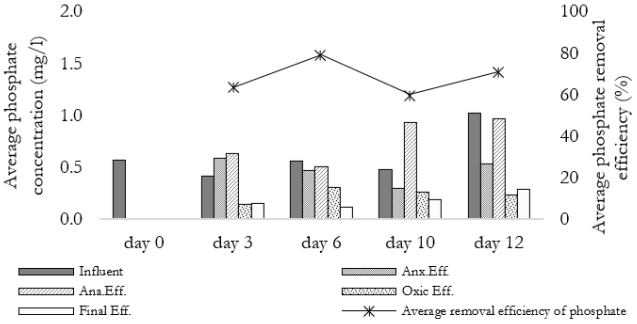

Fig. 5. Phosphate removal performance.

The more intriguing aspect of our phosphate result was the reduction in phosphate concentrations from 0.48-1.02 mgPO_4-P/l to 0.30-0.53 mgPO_4-P/l after the water passed through the anoxic tank. This implied the presence of denitrifying phosphorus accumulating organisms (DPAOs), which can accumulate phosphate in anoxic conditions by using nitrate or nitrite as an electron acceptor rather than oxygen [24]. The presence of DPAOs was also supported by the direct variation in nitrate and phosphorus removal rates shown in Fig. 8. However, further biological community analysis is required to confirm the presence of DPAOs.

Although the system was unable to reduce TAN and nitrate at the start of the treatment period, removals finally occurred on the sixth and third days of the operation, with efficiencies of 57-82% and 14-52%, respectively (see Fig. 5-6). TAN concentrations in the effluent ranged from 0.70±0.055 to 1.96±0.002 mg TAN-N/l, which were acceptable for aquatic-life criteria (22 mg/L at pH 7 [25]), but nitrate concentrations in the effluent ranged from 0.14±0.004 to 3.46±0.078 mgNO_3-N/l, which were higher than the suggested level for the most sensitive freshwater species (2.0 mgNO_3-N/l [26]. Because TAN was primarily removed in an oxic tank and its removal rates increased as the nitrate removal rate increased (Fig. 8), nitrification may be the primary process for TAN removal. Denitrification in our system occurred primarily in the oxic tank (days 3rd, 6th, and 12th), while it was observed in the anoxic tank only on the 12th day of treatment (Fig. 7). This suggested the presence of aerobic denitrifiers in the oxic tank, similar to those found in Wen and Wei's A2O treatment system [27], rather than conventional anoxic denitrifiers in the anoxic tank.

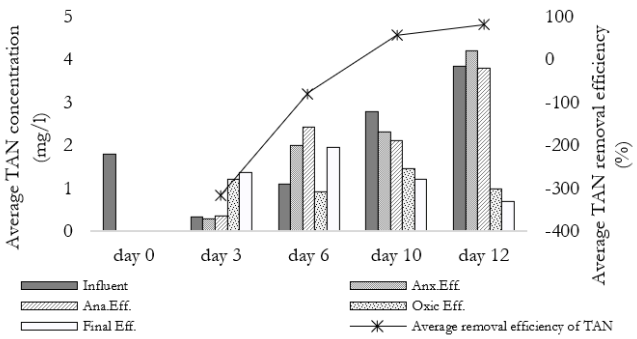

Fig. 6. TAN removal performance.

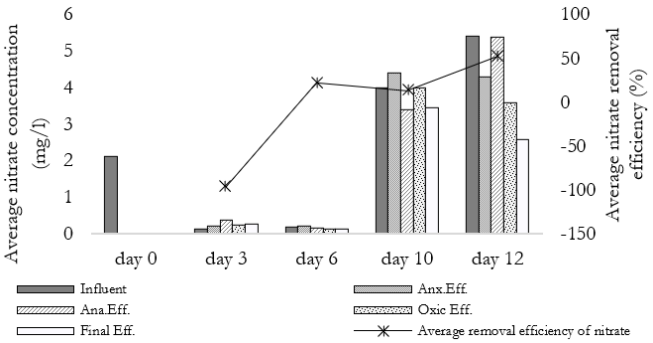

Fig. 7. Nitrate removal performance.

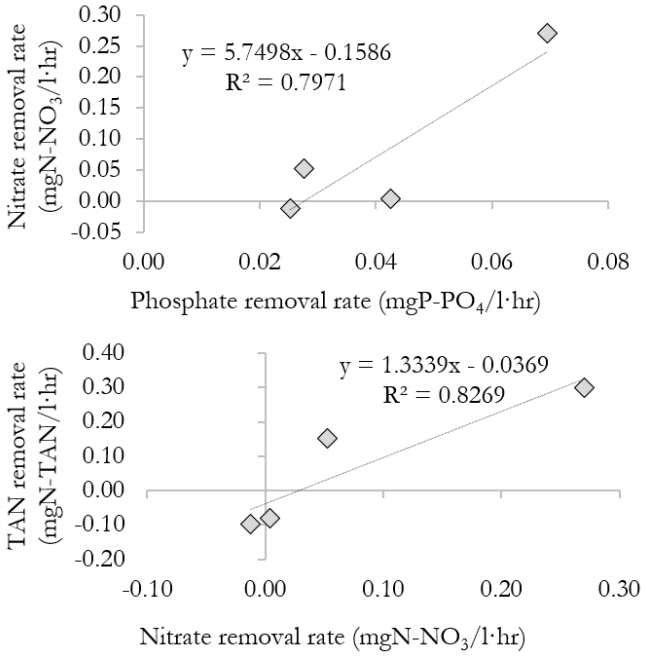

Fig. 8. Relationship between removal rates.

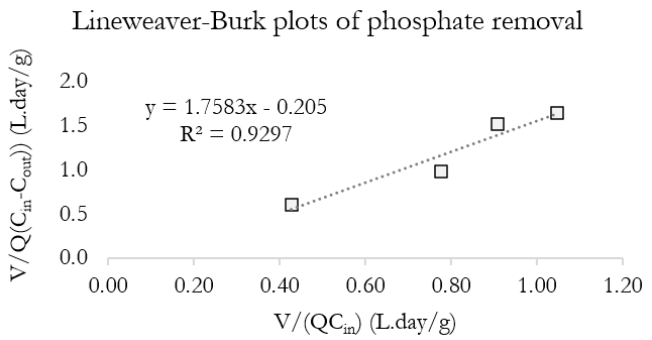

Fig. 9. Kinetic analysis of phosphate removal.

The Lineweaver-Burk plots shown in Fig. 9 were used to perform a kinetic analysis of phosphate removal. Phosphate removal rates of the reverse A2O–MFC system ($Q(C_{in} - C_{out})/V$) decreased as phosphate loading rates (QC_{in}) decreased and could be estimated using the equation shown in Fig. 8 with a coefficient of determination of 0.930. According to the equation, if the influent contains 0.7 mg PO_4-P/l phosphate, the total volume of the reverse A2O–MFC system must be increased by 200% to achieve 0.05 mg PO_4-P/l phosphate in the final effluent.

The average removal rates at the open circuit operation (day 20 - day 36 of the start-up period) and the closed circuit operation (day 3 - day 12 of the treatment period) were calculated to discuss the effect of MFC on pollutant removals (Table 3). Based on a one-tailed t-test (p-value=0.038, significance level =0.05), the average COD removal rate at the closed circuit operation (66.34±16.59) was significantly higher than that of the open circuit operation (27.4±17.04). This finding suggested that embedding an MFC in the reverse A2O process could improve COD removal performance. There has yet to be published research that integrates MFC technology with the reverse A2O process.

This finding, however, was not surprising given that a few studies had suggested that embedding an MFC in an A2O process could improve pollutants removal [9, 10, 11]. Xie et al. demonstrated that the COD, total nitrogen (TN), and total phosphorus (TP) removal efficiencies of the MFC-A2O reactor increased by 15.9%, 9.3%, and 1.4%, respectively, when compared to the controlled A2O reactor [9]. They believed that the electrochemical reaction catalyzed by microorganism electrogenesis was the primary factor for COD removal enhancement in the MFC-A2O reactor [9]. Xie et al. discovered that the microbial community structures on the surface of the cathode and in the suspensions of the cathode chamber in the MFC-A2O reactor have changed by comparing microbial community structure in the A2O reactor with or without MFC [11]. The percentage of denitrifying bacteria in the suspension liquid increased significantly when the MFC was embedded in the A2O reactor [11]. Bacteria from the genus *Rheinheimera* were also enriched on the cathode surface, which may contribute to nitrogen removal [11]. For TP removal enhancement, Li et al. explained that bio-cathodes could ease competition for carbon between phosphorus and denitrification in a certain extent and were helpful for anaerobic phosphorus' release [11]. However, no significant improvement in nitrate, TAN, or phosphate removal from the reverse A2O-MFC system was found in this study.

Table 3. Pollutant removal rates at the open circuit operation and the closed-circuit operation of the reverse A2O–MFC system.

Removal rate (mg/L·h)	Open circuit operation	Closed circuit operation
COD	22.07 ± 17.56	66.34 ± 16.59
Phosphate	0.03 ± 0.04	0.04 ± 0.02
TAN	0.005 ± 0.02	0.07 ± 0.17
Nitrate	0.23 ± 0.50	0.08 ± 0.11

3.2. Electricity Generation Performance

3.2.1. Open circuit voltage (OCV) during the treatment period

The potential for electricity generation was demonstrated by OCV data (Fig. 10) measured at each electrode-placement pattern. The highest OCVs were observed in group 2, namely CH04 = 707.35 mV, CH05 = 718.91 mV, and CH06 = 7103.32 mV, followed by those in group 3, namely CH07 = 6026.28 mV, CH08 = 6843.9 mV, and CH09 = 6484.56 mV. Group 1 had the lowest OCVs: CH01 = 38.415.4 mV, CH02 = 34.812.7 mV, and CH03 = 16.72.27 mV. ORP data measured at the anode and cathode chambers could explain this. The difference in electrical potential between an anode and a cathode installed in the anaerobic tank and the oxic tank was reasonably the highest in group 2 (CH04-CH06), due to the fact that the ORPs in the anaerobic tank (-228-66 mV) were much lower than those in the oxic tank (70-110 mV). The difference in electrical potential between an anode and a cathode installed in the anoxic tank and the oxic tank was rationally lower in group 3 (CH07-CH09) than in CH04-CH06 due to smaller ORPs difference between an anoxic tank (-98-72 mV) and the oxic tank (70-110 mV). In group 1, the lowest ORP difference between an anode and a cathode placed in the anaerobic tank (-228-66 mV) and the anoxic tank (-98-72 mV) could explain their lowest OCVs at CH01-CH03. However, the condition in closed electrical circuits may change due to the actual movement of ions in the electrical wire and those in the water flow.

DOI:10.4186/ej.2022.26.10.11

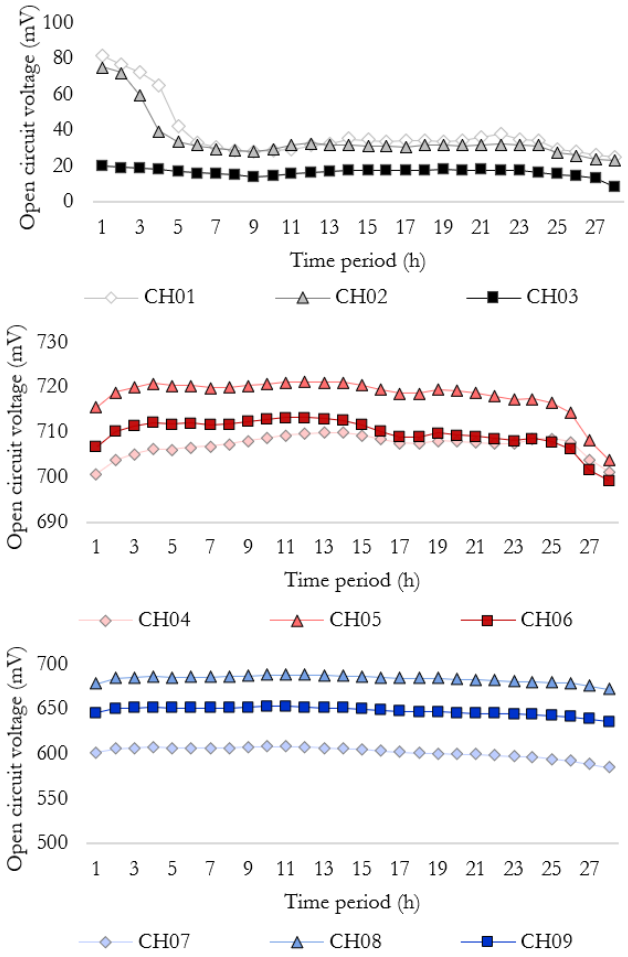

Fig. 10. OCV during the treatment period.

3.2.2. Closed circuit voltage (CCV) during the treatment period

According to the first polarization experiment during the 29th-30th hour of the treatment, External resistors of 10,000 ohms, 47,000 ohms, 47,000 ohms, 47,000 ohms, 47,000 ohms, 5100 ohms, 100 ohms, 47,000 ohms were selected for CH01, CH02, CH03, CH04, CH05, CH06, CH07, CH08, and CH09, respectively. It was previously established that the external resistance that provides maximum power output equals the internal resistance [28]. As a result, the resistance value mentioned above also indicated the internal resistance of each electrical circuit. The electrical current flowed with various CCVs after connecting each selected external resistor to each anode-cathode pair, were shown in Fig. 11.

During the 31st-121st hours of the treatment period, the CCVs of each electrode-placement pattern were 23.43.97 mV for CH01, 46.1±13.7 mV for CH02, -52.3±19.8 mV for CH03, 236±51.0 mV for CH04, 319±16.9 mV for CH05, 89.5±12.8 mV for CH06, -3.94±1.17 mV for CH07, 0.033±0.020 mV for CH08, and -29.3±16.7 mV for CH09. The absolute value of CCVs was found to be highest at CH05 and lowest at CH08. This could be explained by the assumption that the electrode-placement patterns of group 2 (CH04-CH06) allowed protons to flow from an anode chamber (the anaerobic tank) to a cathode chamber (the oxic tank). As a result, CH04-CH06 may contribute to high electrical voltages. Lower voltages were understandable given that the electrode-placement patterns of group 1 (CH01-CH03) could result in the loss of protons from a cathode chamber (anoxic tank) to an anode chamber (anaerobic tank) via water flow. The longest distance (50-90 cm) between each anode-cathode pair in group 3 (CH07-CH09) compared to the other two groups could result in the loss of electrons and protons during the system flow from an anode chamber (anoxic tank) to a cathode chamber (oxic tank).

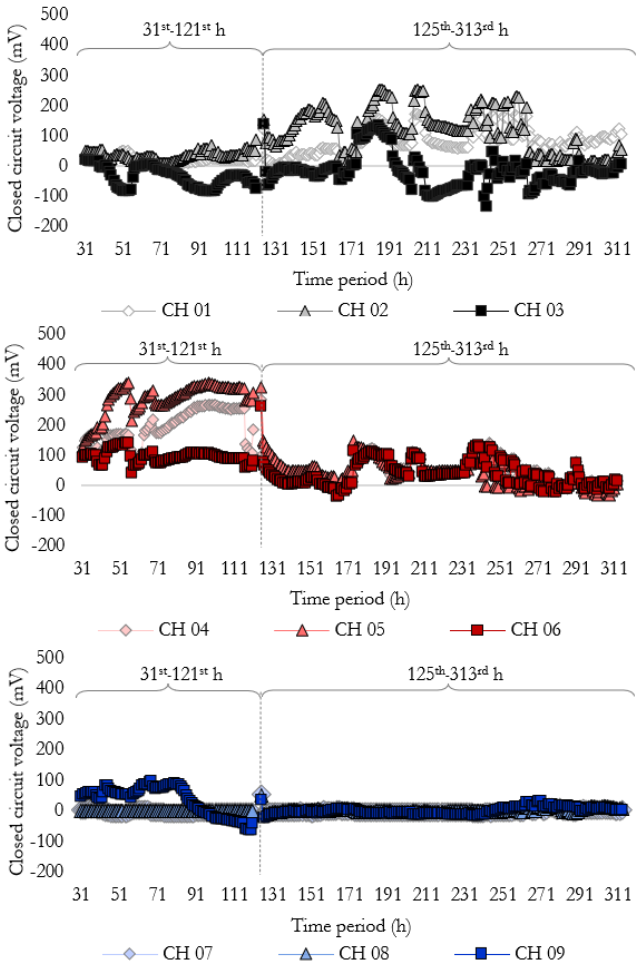

Fig. 11. CCV during the treatment period.

For the second polarization experiment during 120th-124th h of the treatment period, external resistors of 47,000 ohms, 5,100 ohms, 47,000 ohms, 50,000 ohms, 50,000 ohms, 47,000 ohms, 5,100 ohms, 10,000 ohms, 10,000 ohms were selected for CH01, CH02, CH03, CH04, CH05, CH06, CH07, CH08, CH09, respectively. CCVs after connected the newly selected resistors during 125th-313rd hour of the treatment period were 83.3±43.3 mV for CH01, 118±72.4 mV for CH02, -14.6±532 mV for CH03, 45.4±41.6 mV for CH04, 42.7±46.9 mV for CH05, 37.6±43.6 mV for CH06, -1.74±6.07 mV for CH07, 1.98±6.72 mV for CH08, 0.509±11.3 mV for CH09, as shown in Fig. 11. While CH09 had the lowest absolute

value of CCVs, CH02 had the highest absolute value of CCVs. One of the possible factors to be discussed in 3.2.3 is a high input of protons to the anoxic tank.

3.2.3. Electrical power generated during the treatment period

Average density of power output during the 31st-121st h of the treatment period was 37.1±34.4 μW/m² (13.4±12.4 μW/m³) for CH01, 18.1±14.3 μW/m² (6.50±5.15 μW/m³) for CH02, 26.5±28.2 μW/m² (9.52±10.2 μW/m³) for CH03, 482±248 μW/m² (173 ±89.3 μW/m³) for CH04, 992±311 μW/m² (357±112 μW/m³) for CH05, 111±46.3 μW/m² (40.1±16.7 μW/m³) for CH06, 3.82±3.14 μW/m² (1.38±1.13 μW/m³) for CH07, 0.089±0.211 μW/m² (0.032±0.076 μW/m³) for CH08, 40.1±30.3 μW/m² (14.4±10.9 μW/m³) for CH09. The highest power output was observed at CH05 between the 31st and 121st hours, as shown in Fig. 12. This corresponded to the highest OCV and CCV of CH05, as shown in Fig. 10-11.

However, as shown in Fig. 12, the highest electrical powers were observed at CH02 during the 125th-313th h of the treatment period. The average power output during the 125th-313th hour of the treatment period was 104±96.1 W/m² (37.4±34.6 W/m³) for CH01, 2088±1996 μW/m² (752±719 μW/m³) for CH02, 35.8±51.8 μW/m² (12.9±18.7 μW/m³) for CH03, 42.1±79.5 μW/m² (15.1±28.6 μW/m³) for CH04, 44.6±97.6 μW/m² (16.1±35.1 μW/m³) for CH05, 39.0±75.2 μW/m² (14.0±27.1 μW/m³) for CH06, 4.32±24.6 μW/m² (1.56±8.85 μW/m³) for CH07, 2.71±10.0 μW/m² (0.977±3.59 μW/m³) for CH08, 7.08±10.5 μW/m² (2.55±3.79 μW/m³) for CH09.

The decreasing of internal resistance at CH02 as its suitable external resistance changed from 47,000 ohms (31st-121st h) to 5,100 ohms (125th-313th h) is one possible reason for CH02 becoming the maximum electricity generator during the 125th-313th h. Possible assumptions for ion flow at CH05 and CH02 were given. In the case of CH04-CH06, protons in the anode chamber (the anaerobic tank) could naturally flow to the cathode chamber (the anoxic tank) to react with oxygens and electrons transferred via the electrical circuit. It was reasonable for them to produce a high power output. However, the electrode distance of CH04 may be so close that an electron flow short circuit occurs directly along with the water flow. Furthermore, the electrode distance of CH06 may be so great that only a few protons can reach the cathode in a given time. As a result, the CH05 with a medium electrode distance produced the highest power output during the 31st-121st h. In the case of CH01-CH03, the loss of protons from the cathode chamber (an anoxic tank) could easily occur along with the water flow. However, if the raw duck pond water that entered an anoxic tank during the 125th-313th hours of treatment contained enough positive ions, high power output at those channels was also possible. More research is needed to prove this assumption.

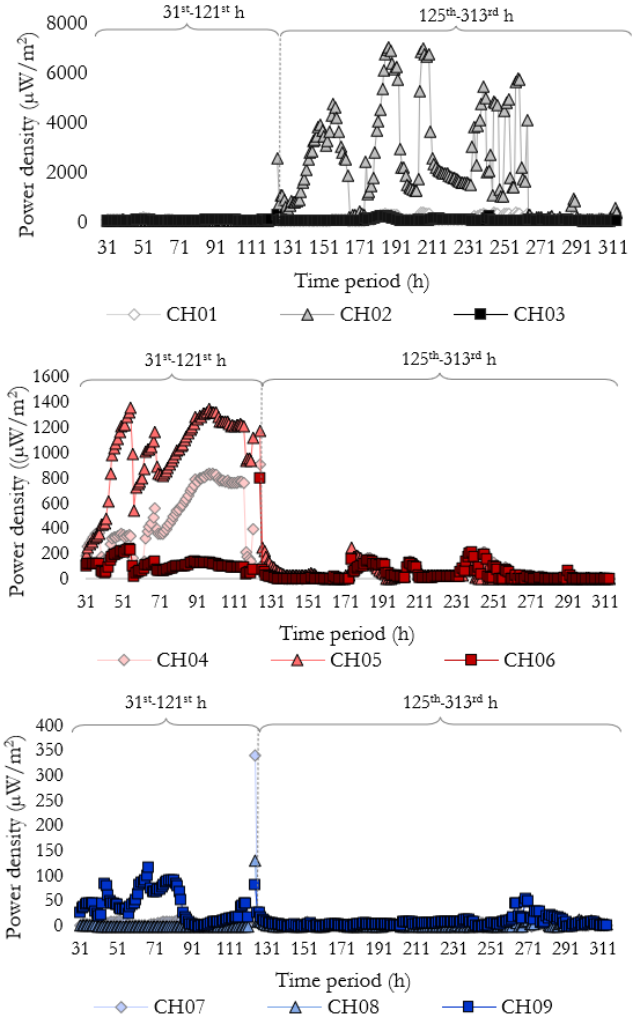

Fig. 12. Power density during the treatment period.

3.2.4. Electrical energy during the treatment period

The total electrical energy (EE) for each electrode-placement pattern was calculated using the previously described Eq. (5) to compare the electrical performance of CH01-CH09.

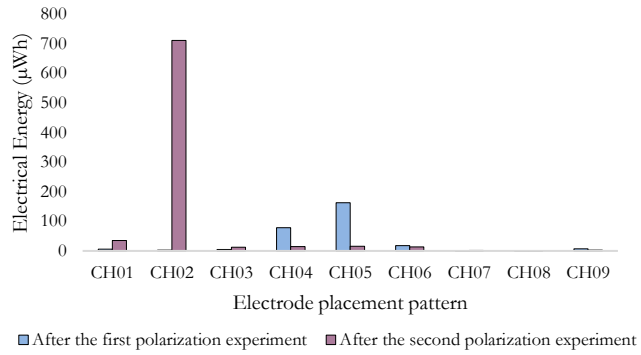

Fig. 13. Electrical energy during the treatment period.

As shown in Fig. 13, CH05 had the highest EE during the 31st-121st h of the treatment period (162.5 Wh), while

DOI:10.4186/ej.2022.26.10.11

CH02 had the highest EE during the 125th-313th h of the treatment period (710.3 Wh). This result is consistent with the power output result described in 3.2.3. It was discovered that the produced electrical energy decreased with operation time for groups 2 (CH04-CH06) and 3 (CH07-CH09). On the other hand, the electrical energy of group 1 (CH01-CH03) increased as the operation time increased. This result indicated the need for additional research into electrode surfaces and electrolytes in both anode and cathode chambers.

3.2.5. Relationship between pollutant removal rates and electricity production

Figure 14 depicts the relationship between COD removal rate and P data for CH01-CH09. P values at CH01 clearly decreased as COD removal rates increased. However, at CH07-CH08, increasing P trends were observed in conjunction with increased COD removal rates. The result implied a variety of possibilities, including competition between non-exoelectrogens and exoelectrogens on anode surfaces, deterioration of electrode conductivity, and an increase in the thickness of suspended solid on the electrode surface. Due to the relatively high power output at CH01, the non-exoelectrogens may largely suspend in the anolyte, while the exoelectrogens formed the biofilm on the anode surface. As a result of the non-exoelectrogens multiplying and increasing the COD removal rate, some of them may become attached to the anode surface, resulting in a decrease in power output. Because of the low power output range of CH07-CH08, there may be a small amount of exoelectrogens on the anode surfaces. Exoelectrogens that bred can cause higher COD removal rates as well as the formation of a biofilm on the anode surface. As a result, the power output rises. Furthermore, suspended solid sedimentation could occur at both the anode and cathode surfaces over time. This could lead to a decrease in conductivity at each electrode surface, which would reduce power generation. These factors could explain the erratic power output trends at CH02-CH06 and CH09.

Figure 15 depicts the relationship between phosphate removal rate and P data for CH01-CH09. When phosphate removal rates increased, decreasing trends in P data were observed at CH03-CH06. If struvite crystallization occurred in the oxic tank for CH04-CH06 cathodes, the phosphate reduction could result in an increase in struvite crystals accumulated on the cathode surfaces. As a result, the cathode's internal resistance may increase. This could result in a reduction in power output at CH04-CH06. Only one case (CH08) in Fig. 15 showed an increase in P data as the phosphate removal rate increased. This could be explained similarly to the COD removal rate and P data in CH08 (Fig. 14). Despite the fact that the above assumptions have not been proven, this relationship is interesting.

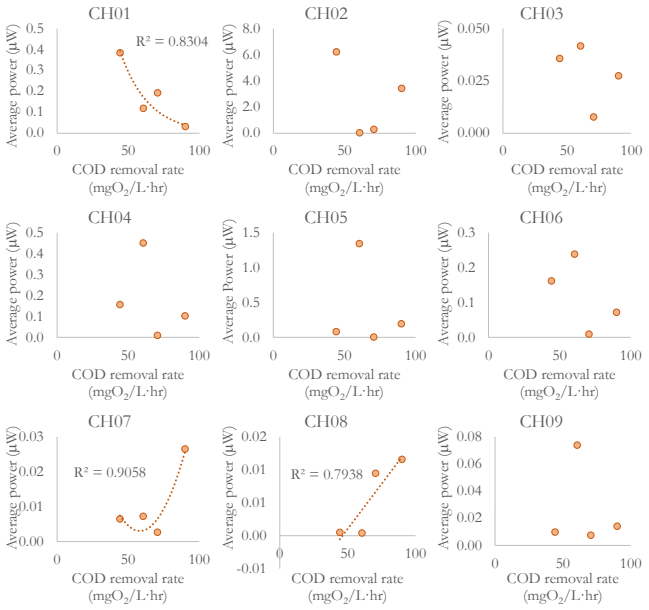

Fig. 14. Relationship between COD removal rate and power output.

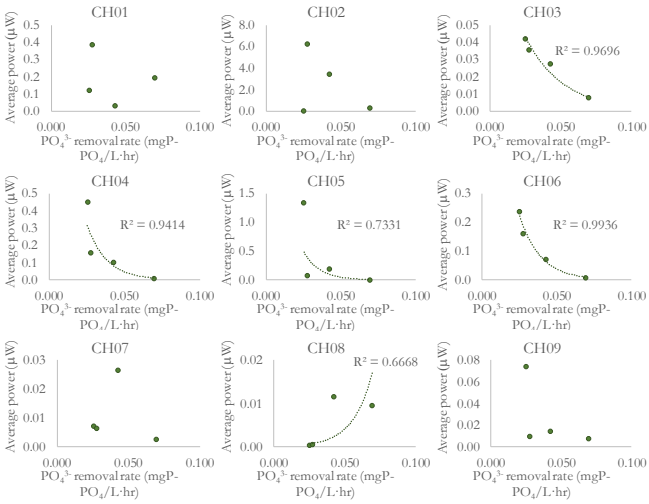

Fig. 15. Relationship between phosphate removal rate and power output.

3.2.6. Aspects for improvement

Polarization curve results (see Fig. 16-17.) indicated critical points for configuration improvement. The doubling back of curves in Fig. 16-17 demonstrated power overshoot, which could occur primarily in cases of mixed consortia inoculum and insufficient separation of anode and cathode [29] due to our reactor design. Furthermore, fermentation, which could occur concurrently with the anodic bioelectrochemical reaction, current leakage, and gas or substrate crossover were all potential causes of power overshoot [29]. Some aspects, such as the mixed consortia inoculum, the parallel fermentation to the anodic bioelectrochemical reaction, and the gas or substrate crossover process, are unavoidable in real-world treatment applications. However, adequate separation of

the anode and cathode, as well as the prevention of current leakage, should be greatly improved in our future work.

In the graphs of CH03, CH07, CH08, and CH09, minus voltage and minus current indicated the reverse flow of electrons from cathodes to anodes at a very low power output. Anodes were placed downstream in the case of CH01-03, so electrons must flow against the water flow to generate electricity. Electrons may be lost along the way if the electrode distance is too long (as in the case of CH03). Because protons from a cathode chamber naturally flow to an anode chamber via the water flow, the cathode chamber most likely contained a higher electron concentration than the anode, allowing it to function as an anode at a very low power output. As a result, low levels of reverse current and voltage were possible. In the case of CH07-09, an excessively long electrode distance should be avoided because it can slow down and reduce electron flow from anodes to cathodes. As a result, a small number of electrons were occasionally allowed to flow backwards from cathodes to anodes. This result suggested that the appropriate electrode distance in our MFC configuration be no more than 45 cm.

Tables 4 and 5 compared our reverse A2O-wastewater MFC's treatment and power generation performance to that of other systems. Table 4 shows that the reverse A2O-MFC had comparable phosphate removal efficiencies to A2O related systems, as well as LSCFB (Liquid-Solid Circulating Fluidized Bed) and modified OD (Oxidation Ditch) systems. However, the reverse A2O-MFC removed less COD and nitrate than the other systems. More efforts should be made to keep the MLSS concentration in each reactor at the intended level. The effluent of an oxic tank should be recycled to the anoxic tank to improve nitrate removal efficiency.

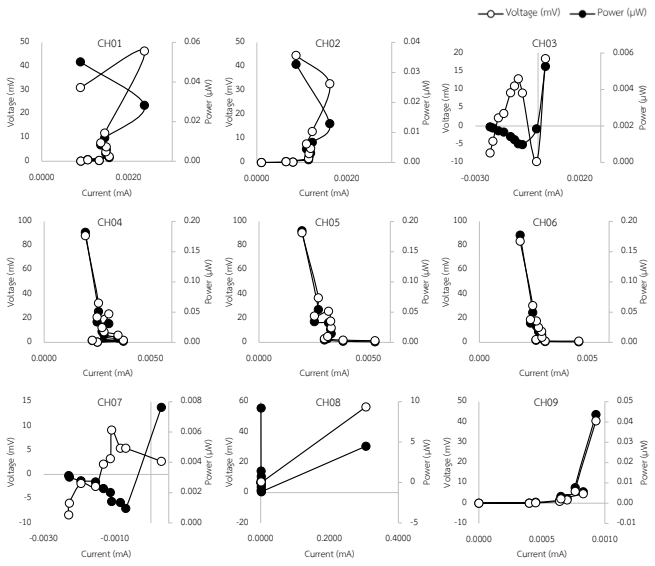

Fig. 16. Result of the first polarization experiment.

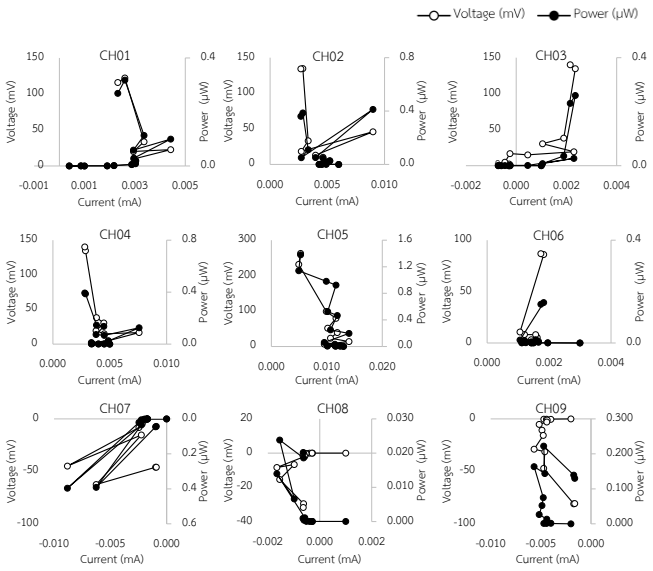

Fig. 17. Result of the second polarization experiment.

Table 4. Wastewater treatment performance of the reverse A2O–MFC comparing to other A2O related systems.

System	Removal efficiencies (%)			COD loading rate (gCOD/L-reactor•d)
	COD	PO_4^{3-} or TP	NO_3^- or TN	
A2O	≥ 90 [30]	PO_4^{3-} 60-71 [30]	NO_3^- 70-85 [30]	-
	92 [10]	TP 45 [10]	TN 80-88 [10]	-
A2O–MFC	94-95 [10]	TP 57-61 [10]	TN 87-88 [10]	
	90 [31]	TP 70 [31]	-	1.573 [31]
Reverse A2O	92 [31]	TP 75 [31]	-	1.360 [31]
	8-50 *	PO_4^{3-} -6 to 38 *	NO_3^- -15 to 29 *	1.412 - 2.258 *
Reverse A2O–MFC	50-82 *	PO_4^{3-} 60-79 *	NO_3^- 14-52*	1.412 - 2.258 *
LSCFB	89-92 [32]	PO_4^{3-} 64-74 [32]	NO_3^- -1075 to -300 [32]	0.052-4.12 [32]
Modified OD	-	TP 27.9-63.9 [33]	-	0.15-0.21[33]
	-	TP 72-75 [34]	TN 70-80[34]	-
		TP 96-97 [34]	TN 80-90[34]	
UASB	75-90 [35]	-	-	13 – 30 [35]
AF	75.9-91.9 [36]	-	-	5 – 17.5 [36]

* : This study, LSCFB : Liquid-Solid Circulating Fluidized Bed, OD : Oxidation Ditch, UASB: Upflow Anaerobic Sludge Blanket Reactor, AF : Anaerobic Filter

Our reverse A2O-MFC produced 0.01510-3 mW/gCOD-removed of electrical energy, which was significantly less than the energy produced by single chamber-air cathode MFCs (anaerobic digestion occurs in anode chambers). Furthermore, our reverse A2O-MFC

system consumed 10 million times more power than it produced during operation (see Table 6). This result indicated the need to improve both electrical production and energy consumption. For example, the electrode installation design, adequate separation of the anode and cathode, and current leakage prevention should all be reconsidered. Furthermore, using a lower powered air pump may reduce the power consumption. A lower powered air pump would suffice for our oxic tank if we used a high efficiency air nozzle instead of the one used in the experiment. As a result, energy consumption may have been reduced.

Assuming a 35% electrical conversion efficiency, 1 m^3 biogas will yield 2.14 kWh of electricity and 1 m^3 methane will yield 10 kWh (10 Wh/L methane gas) [40]. As a result, the UASB (Upflow Anaerobic Sludge Blanket Reactor) and AF (Anaerobic Filter) in Table 5 can produce electricity of 20×10^6 to 28×10^6 mWh/kg removed COD and 28×10^6 mWh/kg removed COD, respectively. Based on the information presented above, UASB [35] and AF [36] can generate more than a thousand times the electrical energy that a single cell MFC can produce.

However, this is not to say that MFC technology is without hope. In fact, MFC technology can be integrated with other existing biological treatment processes to directly harvest byproduct electrons and generate additional electrical energy. When Gong et al treated oilfield wastewater with a microbial fuel cell integrated with an up-flow anaerobic sludge blanket reactor, they obtained a maximum power density of 93 mW/m2 [41]. At 26 hours HRT, their UASB-MFC system removed more than 90% COD and 83% NH3-N from oilfield wastewater [41]. Zhang et al. created an up-flow anaerobic sludge blanket reactor-microbial fuel cell-biological aerated filter (UASB-MFC-BAF) system for simultaneous bioelectricity generation and molasses wastewater [42]. When high strength molasses wastewater with 127,500-mg/l COD was used as the influent, they obtained a maximum power density of 1410.2 mW/m^2 and a current density of 4947.9 mA/m^2 [42]. The total COD, sulfate, and color removal efficiencies of the UASB-MFC-BAF were 53.2%, 52.7%, and 41.1%, respectively [42]. Furthermore, MFCs can be connected in a stacked configuration to improve performance. Ge et al. designed and installed a 200-L stacked MFC with 96 tubular MFC cells in a local wastewater treatment plant (Pepper's Ferry Regional Wastewater Treatment Authority, Radford, VA) [43]. The system was operational for over 300 days [43]. By continuously treating the primary effluent at an HRT of 6-12 h and storing the energy extracted from the MFC system in 5 V capacitors, the produced energy could be used to power the water pump via a 3-12 V boost converter [43]. It took 50-60 minutes to charge the capacitors from 4 to 5 V, while a 1 V drop could provide enough energy to run the water pump for catholyte recirculation for about 5 seconds [43]. In comparison to the previous works, the reverse A2O-MFC in this study is only the first step in providing information and encouragement to researchers interested in integrating new ideas with existing systems for more energy sustainability.

Table 5. Comparison of electricity generation performance among A2O–MFC systems, reverse A2O–MFC system, and other systems.

Systems	Methane yields (L-CH_4 /kg-COD removed)	Normalize energy recovery (mWh/g-COD removed)
Single chamber-air cathode MFC	-	148±0.007 [37]
	-	220-750 [38]
	-	1,950 [39]
Reverse A2O–MFC	-	0.015×10^{-3} *
UASB	200-280 [35]	-
AF	250-[36]	-

Table 6. Power consumption and power output of the reverse A2O–MFC system.

Item		31-121 h	125-313 h
Consumed power (μW)	Influent (Main pump)	12×10^6	12×10^6
	Anx. Tank (Stirring motor)	0.12×10^6	0.12×10^6
	Ana. Tank (Stirring motor)	0.12×10^6	0.12×10^6
	Oxic tank (Aeration pump)	25×10^6	25×10^6
	Total	**37.24×10^6**	**37.24×10^6**
Average power output (μW)	CH01	0.067	0.187
	CH02	0.033	3.758
	CH03	0.048	0.064
	CH04	0.867	0.076
	CH05	1.786	0.080
	CH06	0.200	0.070
	CH07	0.007	0.008
	CH08	0.000	0.005
	CH09	0.072	0.013
	Total	**3.08**	**4.261**

4. Conclusion

A reverse-A2O MFC was designed and tested in duck pond water as the first step in the reverse A2O-MFC study. It was possible to achieve phosphate removal efficiencies of 60-79%, COD removal efficiencies of 50-85%, and TAN removal efficiencies of 57-82%. Because of the residual dissolved oxygen in an anoxic tank, the nitrate removal was relatively low (14-52%). Phosphate removal rates decreased as phosphate loading rates decreased, and they could be estimated using Lineweaver-Burk plots with a coefficient of determination of 0.930. When an anode and a cathode were installed in an anaerobic tank and an oxic tank, respectively, with an electrode distance of 35 cm (CH05), our reverse A2O-MFC generated the highest electrical energy of 162.5 Wh between the 31st and 121st

hours of the treatment period. During the 125th-313th hours of treatment, however, the highest electrical energy of 710.3 Wh was detected at another circuit in which an anode and a cathode were installed in an anaerobic tank and an anoxic tank, respectively (CH02), with an electrode distance of 35 cm. Miscellaneous aspects, such as the inspection of electrode surfaces and electrolytes in both anode and cathode chambers at the end of the experiment, as well as the biological community analysis for the presence of DPAOs and oxic denitrifiers, are required to further explain the result.

Acknowledgement

We would like to express our heartfelt gratitude to everyone who helped us complete this study. We were grateful to Mr. Khajornsak Saeteng for donating his farm area, pond water, and electricity to our experiments. We also thanked Assoc. Prof. Dr. Chontisa Sukkasem for her insightful comments on our work. Finally, we would like to thank Mahasarakham University for funding this research study.

References

[1] B. T. G. Balasuriyage, H. G. Shabbir, and P. Trakarn,. "Aquatic eutrophication potential of fertilizer application in maize cultivation in Thailand," *Thai Environmental Engineering Journal*, vol. 35, no. 2, pp. 67-79, 2021.

[2] S. Chotpantarat and S. Boonkaewwan, "Impacts of land-use changes on watershed discharge and water quality in a large intensive agricultural area in Thailand," *Hydrological Sciences Journal*, vol. 63, no. 9, pp. 1386-1407, 2018.

[3] J. Rewthong, K. Tungkananuruk, W. Wararam, and N. Semvimol, "Reduction of nitrogen and phosphorus nutrient in retention effluent pond from power plant by adsorption and filter layer," *Thai Environmental Engineering Journal*, vol. 31, no. 3, pp. 35-46, 2017.

[4] R. Prateep Na Talang, S. Sirivithayapakorn, and S. Polruang, "Environmental impacts and cost-effectiveness of Thailand's centralized municipal wastewater treatment plants with different nutrient removal processes," *Journal of Cleaner Production*, vol. 256, p. 120433, 2020, doi:10.1016/j.jclepro.2020.120433.

[5] S. Xu, M. Bernards, and Z. Hu, "Evaluation of Anaerobic/Anoxic/Oxic (A2/O) and reverse A2/O processes in biological nutrient removal," *Water Environment Research*, vol. 86, no. 11, pp. 2186-2193, 2014.

[6] F. Fang, L. -L. Qiao, J. -S. Cao, Y. Li, W. -M. Xie, G. -P. Sheng, and H. -Q. Yu, "Quantitative evaluation of A2O and reversed A2O processes for biological municipal wastewater treatment using a projection pursuit method," *Separation and Purification Technology*, vol. 166, pp. 164-170, 2016.

[7] N. Prasertsung, A. Reungsang, and C. Ratanatamskul, "Alkalinity of cassava wastewater feed in anodic enhance electricity generation by a single chamber microbial fuel cells," *Engineering Journal*, vol. 16, no. 5, pp. 18-27, 2012.

[8] W. Niyom, D. Komolyothin, and B. B. Suwannasilp, "Important role of abiotic sulfide oxidation in microbial fuel cells treating high-sulfate wastewater," *Engineering Journal*, vol. 22, no. 4, pp. 23-37, 2018.

[9] B. Xie, W. Dong, B. Liu, and H. Liu, "Enhancement of pollutants removal from real sewage by embedding microbial fuel cell in anaerobic-anoxic-oxic wastewater treatment process," *Journal of Chemical Technology & Biotechnology*, vol. 89, no. 3, pp. 448-454, 2013.

[10] B. Li, W. Dong, B. Liu, B. Xie, and H. Liu, "Electricity generation performance of microbial fuel cell embedded in anaerobic-anoxic-oxic wastewater treatment process," *Journal of Biosciences and Medicines*, vol. 9, pp. 32-37, 2015.

[11] B. Xie, B. Liu, Y. Yi, L. Yang, D. Liang, Y. Zhu, and H. Liu, "Microbiological mechanism of the improved nitrogen and phosphorus removal by embedding microbial fuel cell in Anaerobic-Anoxic-Oxic wastewater treatment process," *Bioresource Technology*, vol. 207, pp. 109-117, 2016.

[12] P. Choudhury, U. S. Prasad Uday, T. K. Bandyopadhyay, R. N. Ray, and B. Bhunia, "Performance improvement of microbial fuel cell (MFC) using suitable electrode and Bioengineered organisms: A review," *Bioengineered*, vol. 8, no. 5, pp. 1-17, 2017.

[13] American Public Health Association (APHA), *Standard Methods for the Examination of Water and Wastewater*, 22rd ed. Washington D.C.; New York: American Public Health Association, 2017.

[14] U.S. Environmental Protection Agency (USEPA), *Method 350.1 Determination of Ammonia Nitrogen by Semi-Automated Colorimetry, 2nd Revision*. Ohio: Environmental Monitoring Systems Laboratory, Office of Research and Development, 1993.

[15] S. N. Kaul, "Nitrate analysis," in *Water and Wastewater Analysis*. New Delhi, India: Daya Publishing House, 2002.

[16] J. E. Dowd and D. X. Riggs, "Comparison of estimates of Michaelis-Menten kinetic constants from various linear transformations," *The Journal of Biological Chemistry*, vol. 240, no. 2, pp. 863-869, 1965.

[17] G. Schön, S. Geywitz, and F. Mertens, "Influence of dissolved oxygen and oxidation-reduction potential on phosphate release and uptake by activated sludge from sewage plants with enhanced biological phosphorus removal," *Water Research*, vol. 27, no. 3, pp. 349-354, 1993.

[18] M. Zaman, X. Liu, and G. Nakhla, "Impact of dissolved oxygen concentration and DPAOs: Nitrifiers population ratio on nutrient removal in EBPR process," *International Journal of Environmental*

Science and Development, vol. 10, no. 9, pp. 257-260, 2019.

[19] S. Seitzinger, J. A. Harrison, J. K. Böhlke, A. F. Bouwman, R. Lowrance, B. Peterson, and G. V. Drecht, "Denitrification across landscapes and waterscapes: A synthesis," *Ecological Applications*, vol. 16, no. 6, pp. 2064-2090, 2006.

[20] *Quality Criteria for Water*, EPA 440/5-86-001, U.S. Environmental Protection Agency (USEPA), Washington, DC, 1986.

[21] D. W. Litke, "Review of phosphorus control measures in the United States and their effects on water quality," U.S. Geological Survey, Water-Resources Investigations Report 99-4007, 1999. [Online]. Available: https://pubs.usgs.gov/wri/wri994007/ (accessed 27 February 2022).

[22] Q. Tao, J. Luo, J. Zhou, S. Zhou, G. Liu, and R. Zhang, "Effect of dissolved oxygen on nitrogen and phosphorus removal and electricity production in microbial fuel cell," *Bioresource Technology*, vol. 164, pp. 402-407, 2014.

[23] O. Ichihashi and K. Hirooka, "Removal and recovery of phosphorus as struvite from swine wastewater using microbial fuel cell," *Bioresource Technology*, vol. 114, pp. 303-307, 2012.

[24] W. Zeng, L. Li, Y. Yang, X. Wang, and Y. Peng, "Denitrifying phosphorus removal and impact of nitrite accumulation on phosphorus removal in a continuous anaerobic-anoxic-aerobic (A2O) process treating domestic wastewater," *Enzyme Microb. Technol.*, vol. 48, pp. 134-142, 2011.

[25] T. -J. Park, J. -H. Lee, M. -S. Lee, C. -H. Park, C. -H. Lee, S. -D. Moon, and K. -D. Zoh, "Development of water quality criteria of ammonia for protecting aquatic life in freshwater using species sensitivity distribution method," *Science of The Total Environment*, vol. 634, pp. 934-940, 2018.

[26] J. A. Camargo, A. Alonso, and A. Salamanca, "Nitrate toxicity to aquatic animals: A review with new data for freshwater invertebrates," *Chemosphere*, vol. 58, no. 9, pp. 1255-1267, 2005.

[27] Y. Wen and C. H. Wei, "Heterotrophic nitrification and aerobic denitrification bacterium isolated from anaerobic/anoxic/oxic treatment system," *African Journal of Biotechnology*, vol. 10, no. 36, pp. 6985-6990, 2011.

[28] J. M. Kamau, D. N. Mbui, J. M. Mwaniki, F. B. Mwaura, and G. N. Kamau, "Microbial fuel cells: Influence of external resistors on power, current and power density," *J. Thermodyn Catal*, vol. 8, no. 1, p. 1000182, 2017.

[29] L. Koók, N. Nemestóthy, K. Bélafi-Bakó, and P. Bakonyi, "The influential role of external electrical load in microbial fuel cells and related improvement strategies: A review," *Bioelectrochemistry*, vol. 140, p. 107749, 2021.

[30] Y. Ma, Y. Peng, X. Wang, S. Wang, "Nutrient removal performance of an anaerobic-anoxic-aerobic process as a function of influent C/P ratio," *Journal of Chemical Technology & Biotechnology*, vol. 80, no. 10, pp.1118–1124, 2005.

[31] W. M. Xie, R. J Zeng, W. W. Li, G. X. Wang, and L. M. Zhang, "A modeling understanding on the phosphorous removal performances of A2O and reversed A2O processes in a full-scale wastewater treatment plant," *Environmental Science and Pollution Research*, vol. 25, no. 23, pp. 22810-22817, 2018.

[32] N. Chowdhury, G. Nakhla, J. Zhu, and M. Islam, "Pilot-scale experience with biological nutrient removal and biomass yield reduction in a liquid-solid circulating fluidized bed bioreactor," *Water Environment Research*, vol. 82, no. 9, pp. 772–781, 2010.

[33] W. Liu, D. Yang, L. Xu, C. Jia, W. Lu, O. I. Bosire, and C. Shen, "Effect of return sludge Pre-concentration on biological phosphorus removal in a novel oxidation ditch," *Chinese Journal of Chemical Engineering*, vol. 20, no. 4, pp. 747-753, 2012.

[34] P. Noophan, R. Rodpho, P. Sonmee, M. Hahn, and S. Sirivitayaphakorn, "Nutrient removal performance on domestic wastewater treatment plants (full scale system) between tropical humid and cold climates," *Applied Environmental Research*, vol. 40, no. 2, pp. 32-39, 2018.

[35] A. Torkian, A. Eqbali, and S. Hashemian, "The effect of organic loading rate on the performance of UASB reactor treating slaughterhouse effluent," *Resources, Conservation and Recycling*, vol. 40, no. 1, pp. 1–11, 2003.

[36] Y. Chen, B. Rößler, S. Zielonka, A. M. Wonneberger, and A. Lemmer, "Effects of organic loading rate on the performance of a pressurized anaerobic filter in two-phase anaerobic digestion," *Energies*, vol. 7, no. 2, pp. 736-750, 2014.

[37] N. J. Koffi and S. Okabe, "High voltage generation from wastewater by microbial fuel cells equipped with a newly designed low voltage booster multiplier (LVBM)," *Scientific Reports*, vol. 10, no. 1, 2020, doi:10.1038/s41598-020-75916-7.

[38] S. Thakur and B. Das, "Investigation on microbial fuel cells fabricated from recyclable materials for energy generation and wastewater treatment," *Nature Environment and Pollution Technology*, vol. 20, no. 4, pp. 1555-1563, 2021.

[39] A. E. Tugtas, P. Cavdar, and B. Calli, "Continuous flow membrane-less air cathode microbial fuel cell with spunbonded olefin diffusion layer," Bioresource Technology, vol.102, no.22, pp.10425–10430, 2011.

[40] S. Suhartini, Y.P. Lestari, I. Nurika, "Estimation of methane and electricity potential from canteen food waste," *IOP Conference Series: Earth and Environmental Science*, vol. 230, p. 012075, 2019.

[41] D. Gong and G. Qin, "Treatment of oilfield wastewater using a microbial fuel cell integrated with an up-flow anaerobic sludge blanket reactor," *Desalination and Water Treatment*, vol. 49, no. 2012, pp. 272-280, 2012.

[42] B. Zhang, H. Zhao, S. Zhou, C. Shi, C. Wang, and J. Ni, "A novel UASB-MFC-BAF integrated system for high strength molasses wastewater treatment and bioelectricity generation," *Bioresource Technology*, vol.100, pp. 5687–5693, 2009.

[43] Z. Ge and Z, He, "Long-term performance of a 200 liter modularized microbial fuel cell system treating municipal wastewater: treatment, energy, and cost," *Environmental Science: Water Research & Technology*, vol. 2, pp. 274-281, 2016.

Supawadee Siripratum was born in Samutprakan province, Thailand in 1995. She received her Bachelor's degree in environmental engineering from Mahasarakham University, Thailand in 2018. Now she is a Master's degree student in Environmental Engineering program at Mahasarakham University, Thailand.

Her recent publication and presentations included 1) Mongkulphit S., Siripratum S., Chumroen W. and Pengchai P. (2021). Roles of Packed Bed Porosity on Performance of Biofilter Microbial Fuel Cell in Synthetic Landfill Leachate Treatment. GMSARN International Journal. 15(4), 360-365; 2) P. Pengchai, S. Siripratum, K. Phonsombat, I. Khemma, N. Raksa, P. Chaweanghong, A. Rueangsri, and S. Mongkulphit, "Performance of Biofilter-Microbial Fuel Cell in Nongpling Municipal Landfill Leachate Treatment," Proceedings of 53rd Annual Conference of Japan Society on Water Environment, 2019, 174.; 3) S. Siripratum, S. Mongkulphit, W Chumroen, and P. Pengchai, "Ammonia and Nitrate Removal in Start-up Period of Synthetic Landfill Leachate Treatment using Biofilter-Microbial Fuel Cell," Proceedings of 53rd Annual Conference of Japan Society on Water Environment, 2019, 180.

Miss Siripratum and her co-researchers had once won the prize in the Engineering Expo 2017 for their invention "Biobattery for smart city" (https://www.youtube.com/watch?v=kuW41p6EHP0).

Petch Pengchai was born in Khon Kean province, Thailand in 1975. She earned a Bachelor's, Master's, and Ph.D. in urban engineering (environmental sanitary course) from the University of Tokyo in 1997, 1999, and 2002, respectively. Her main focus during her Ph.D. studies is on air pollution.

Her professional experience includes working as a lecturer at Chiang Mai University in Thailand from 2002 to 2008, and as a lecturer at Mahasarakham University from 2008 to the present. She was appointed assistant professor in 2005, based on her work primarily in the field of air pollution. Her major works, however, have been in the field of wastewater treatment using biofilter and microbial fuel cell since 2008. Low-cost technologies such as constructed wetlands and hydroponics are also of interest.

Assistant Professor Pengchai and her co-researchers had once won the prize in the Engineering Expo 2017 for their invention "Biobattery for smart city" (https://www.youtube.com/watch?v=kuW41p6EHP0).